Proc. Natl. Acad. Sci. USA
Vol. 86, pp. 4440–4444, June 1989
Biochemistry

X-ray analysis of D-xylose isomerase at 1.9 Å: Native enzyme in complex with substrate and with a mechanism-designed inactivator

(enzyme mechanism/crystal structure/metals in enzymes/sugar conformation/suicide inhibition)

H. L. CARRELL*†, JENNY P. GLUSKER*, VINCENT BURGER‡, FRANCO MANFRE‡, DENIS TRITSCH‡, AND JEAN-FRANCOIS BIELLMANN‡

*The Institute for Cancer Research, The Fox Chase Cancer Center, Philadelphia, PA 19111; and ‡Laboratoire de Chimie Organique Biologique, Unité Associée–Centre National de la Recherche Scientifique 31, Institut de Chimie, Université Louis Pasteur, 1, rue Blaise Pascal, 67008 Strasbourg, France

Communicated by Irwin A. Rose, March 27, 1989 (received for review February 24, 1989)

ABSTRACT **The structures of crystalline D-xylose isomerase (D-xylose ketol-isomerase; EC 5.3.1.5) from *Streptomyces rubiginosus* and of its complexes with substrate and with an active-site-directed inhibitor have been determined by X-ray diffraction techniques and refined to 1.9-Å resolution. This study identifies the active site, as well as two metal-binding sites. The metal ions are important in maintaining the structure of the active-site region and one of them binds C^3-O and C^5-O of the substrate forming a six-membered ring. This study has revealed a very close contact between histidine and C^1 of a substrate, suggesting that this is the active-site base that abstracts a proton from substrate. The mechanism-based inhibitor is a substrate analog and is turned over by the enzyme to give a product that alkylates this same histidine, reinforcing our interpretation. The changes in structure of the native enzyme, the enzyme with bound substrate, and the alkylated enzyme indicate that the mechanism involves an "open-chain" conformation of substrate and that the intermediate in the isomerization reaction is probably a cis-ene diol because the active-site histidine is correctly placed to abstract a proton from C^1 or C^2 of the substrate. A water molecule binds to C^1O and C^2O of the substrate and so may act as a proton donor or acceptor in the enolization of a ring-opened substrate.**

D-Xylose isomerase (D-xylose ketol-isomerase; EC 5.3.1.5) is a soluble enzyme that catalyzes the conversion of the aldo-sugar D-xylose to the keto-sugar D-xylulose (1), and, more slowly, D-glucose to D-fructose. Only α-anomers are utilized. During catalysis a proton migrates in a completely stereospecific way (no exchange with the medium) between two adjacent carbon atoms, C^1 and C^2 of the substrate (2). The mechanism of this reaction is thought to involve a cis-ene diol intermediate (2). Polyols are good competitive inhibitors (3). Divalent metal ions, Mn, Co, or Mg, are required for catalytic activity (4).

The *Streptomyces rubiginosus* enzyme, M_r ≈173,000 consisting of four identical subunits, crystallizes (5) in the space group $I222$, $Z = 2$ with a single subunit as the asymmetric unit. The unit-cell dimensions are $a = 93.88$, $b = 99.64$, and $c = 102.90$ Å. We have established that each subunit folds as a $(\beta\alpha)_8$-beta-barrel (5–7), as found in several other enzymes (8).

We (at the University of Strasbourg, V.B., F.M., D.T., and J.F.B.) designed and synthesized a substrate analog that is a suicide inactivator, analog **2** (Scheme **1**) (9). It was used to test whether the D-xylose isomerase studied by X-ray diffraction techniques by us (at the Fox Chase Cancer Center, H.L.C. and J.P.G.) is active in crystalline state. Three crystal structures have been determined and each has been refined: native enzyme, enzyme with bound substrate/product, and enzyme after reaction with the mechanism-based inhibitor, analog **2**. Comparisons of these structural results have given information on the mode of action of this enzyme.

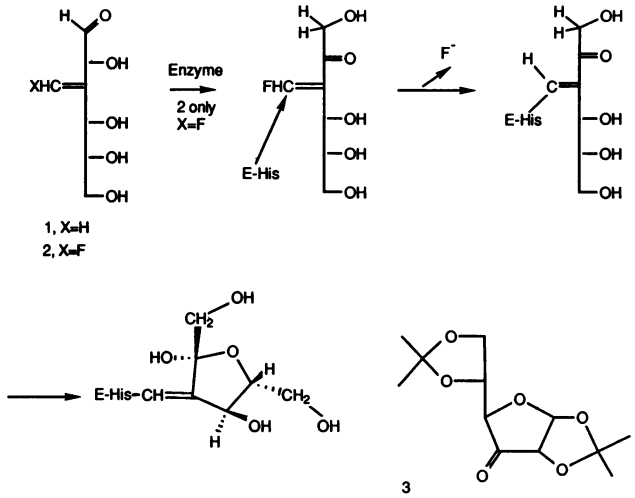

Scheme 1

MATERIALS AND METHODS

Preparation of Active-Site-Directed Inhibitor. 3-Deoxy-C^3-methylene-D-glucose (analog **1**) and (*E*)-3-deoxy-C^3-fluoromethylene-D-glucose (analog **2**) were prepared as follows. Chromic oxidation (10) of the hydroxyl group at C^3 of 1,2:5,6-diisopropylidene-α-D-glucose (11) gave the ketone **3**. The Wittig reaction of ketone **3** with ylide prepared from triphenylmethylphosphonium bromide with potassium *t*-butanolate (12) or with the ylide derived from fluoromethyl triphenylphosphonium tetrafluoroborate (13) with *n*-butyllithium and potassium *t*-butanolate (14) gave, after quantitative acid hydrolysis (15) of the acetonides (16, 17), the glucose analogs **1**§ and **2**¶ (Scheme **1**). Anomers of analogs **1** and **2** were detected in aqueous solutions by NMR spectroscopy.

Assay of Xylose Isomerase. The enzyme from *S. rubiginosus* was assayed by the cysteine–carbazole test (18) as the quantity of D-fructose formed. All reactions were performed in a 0.2 M sodium phosphate buffer (pH 8.0) at 40°C. The reaction mixture (1 ml) contained 0.8 M glucose, 0.01 M

The publication costs of this article were defrayed in part by page charge payment. This article must therefore be hereby marked "*advertisement*" in accordance with 18 U.S.C. §1734 solely to indicate this fact.

†To whom reprint requests should be addressed.

§In a total yield of 80%: m.p. 123–125. ^{13}C-NMR (50 MHz, ^2H_2O) δ (ppm): 148; 146.4; 98.8; 93.0; 80.1; 74.7; 73.3; 70.7; 68.3; 61.9. $[\alpha]_D^{22}$ +72.0° (1.0%, H_2O after 24 hr).

¶Beside the (*Z*)-isomer in the ratio *E*:*Z* = 4:1 in a total yield of 55%. For the stereochemistry, see ref. 17. (*E*)-Isomer is an oil; ^{19}F NMR [376 MHz; $(C^2H_3)_2Eo$] δ (ppm; $CFCl_3$ internal reference): −124.6 (d); −130.5 (d); −132.0 (d); −132.5 (d) with $J_{F,8}$ 82.8 Hz $[\alpha]_D^{22}$ + 101.2° (1.0%, H_2O after 24 hr).

$MgCl_2$, and 2.85 mg of enzyme. The reaction was slowed by diluting 4 μl of the mixture with 1 ml of water and the concentration of D-fructose was immediately determined. The inactivation of xylose isomerase (2.85 mg/ml) by analog **1** (0.4 to 1 M) and analog **2** (0.04 to 0.4 M) was studied in the presence of 0.01 M $MgCl_2$. At given times, aliquots were withdrawn and the residual enzymic activity was measured. The inactivation of xylose isomerase by analog **2** was monitored by ^{19}F NMR. The enzyme (56 mg, 1.3 μmol in subunit) was incubated with analog **2** (3.2 μmol) in a 0.01 M $MgCl_2$ under the conditions listed above (total volume = 0.5 ml). The spectra were recorded after 0, 2, 6, and 24 hr. Trifluoroacetic acid was used as internal standard for the quantitative determination of fluoride ion release.

Preparation of Crystals and X-Ray Diffraction Data Collection. The solution used to prepare crystals contained purified D-xylose isomerase at ≈25 mg/ml, 0.76 M $(NH_4)_2SO_4$, and 0.01 M Pipes (pH 7.4). The solution was refrigerated overnight at 4°C and crystals, as large as ≈2 mm, formed. Native enzyme solution, stored only in water at 4°C at ≈80 mg/ml, was shown by G. D. Markham of this institute using EPR spectroscopy to contain two Mn^{2+} per subunit. Crystals of the native enzyme deteriorated rapidly in the x-ray beam but were stabilized by adding $MgCl_2$. The crystals of enzyme with bound substrate/product were prepared by placing native crystals in a droplet containing D-xylose at 1 M concentration and allowing them to equilibrate for 2 days at 4°C. Crystals of the enzyme containing the active-site-directed inhibitor, analog **2**, were prepared by placing crystals in a droplet containing crystallization mother liquor containing analog **2** at a concentration of about 2 mM plus both Mn^{2+} and Mg^{2+} at 2 mM and soaking them in this manner at 4°C for 4 days. In all cases, the pH of the mother liquor was maintained at 7.4–7.6.

The x-ray diffraction data were measured, to a resolution of 1.9 Å (see Table 1), at 12–15°C using a Nicolet/Xentronix area detector mounted on a Rigaku rotating anode generator and with Ingersoll–Rand focusing nickel mirrors. The data were processed using the XENGEN software package (19). Two crystals of each were used in the data collections of native enzyme and crystals soaked in D-xylose (149,256 and 159,282 data, respectively, before merging). Only one crystal was used for the study of the complex of enzyme with analog **2** (71,368 reflections). R_{merge} values ranged from 0.062 to 0.064.

The structure of the native enzyme at both 4-Å and 3-Å resolution has been published by us (6, 7). The electron density map at 2.5 Å was calculated using phases that resulted from the extension of the isomorphous replacement phases utilizing solvent-flattening techniques (20). A known amino acid sequence (21) was then fit to this map using the computer-graphics system FRODO (22). The metal ions were located in the enzyme using the known stereochemistry of metal–carboxylate interactions (23).

Table 1. Summary of data collections and refinement

Data	Enzyme		
	Native	Native + D-xylose	Native + analog **2**
Crystal type			
a (Å)	93.9	94.2	93.8
b (Å)	99.7	100.2	100.0
c (Å)	102.9	103.2	103.0
No. of unique data/ % of data expected	35,493/91	38,364/98	36,274/94
No. of data with $I > 1.5\sigma(I)$	28,313	30,656	30,250
Total no. of atoms/ no. of H_2O	3,357/306	3,353/291	3,362/299
$R = \sum \lvert F_0 - F_c \rvert / \sum \lvert F_0 \rvert$	0.131	0.141	0.141

F_0, observed structure factor; F_c, calculated structure factor.

Refinement. The structure was refined using restrained least squares refinement (24, 25) accelerated by the use of fast Fourier transforms (26) as implemented by Knossow *et al.* (27). The initial refinement proceeded with several model rebuilding steps with FRODO utilizing $(2F_{obs} - F_{calc})$ maps as well as $(F_{obs} - F_{calc})$ maps. The refinement of the native enzyme (Table 1) converged to $R = 0.22$ at which time solvent molecules were included in the refinement. In all three of the structures, the highest value for the subsequent difference electron density was 0.33 electrons per $Å^3$ (≈4.5 times the estimated standard deviation in the electron density). For the restrained refinements, the rms deviations from ideal geometry ranged from 0.022 to 0.023 Å in bond distances and from 0.041 to 0.045 Å in one to three neighbor distances. The average overall temperature factor ranged from 19 to 22 $Å^2$ from Wilson statistics. In all three refinements, individual temperature factors were restrained to fall no lower than $B = 6$ $Å^2$. The average main-chain isotropic temperature factors for the three refinements ranged from 11 $Å^2$ for native enzyme to 17 $Å^2$ for the xylose-soaked crystals. Analysis of the results using the method of Luzzati (28) indicates that the rms error in coordinates is ≈0.15 Å.

RESULTS AND DISCUSSION

Features. The four subunits of the *S. rubiginosus* enzyme are related by three mutually perpendicular crystallographic twofold axes. Each subunit contains two structural domains, the first having the $(\beta\alpha)_8$ motif (residues 1–323), and the second consisting of a loop of 65 residues that form a series of small interconnected helices. The second-domain loop interacts with the first domain of another subunit of the same molecule (related by the twofold axis that is coincident with the crystallographic *a*-axis) to give a dimer of subunits locked in a mutual "one-armed embrace." Operation of the twofold axis conicident with the *b* (or *c*) crystallographic axis then produces the tetrameric molecule. The structure contains a cis peptide linkage between Glu-186 and Pro-187. This may form a rigid unit necessary to maintain the structural integrity of the active site. Three hundred six solvent sites were located. Details of the structure will be published elsewhere.

Metal Binding. The metal cations were located in the native enzyme structure as outlined (23) by carefully analyzing the potential binding sites with respect to predictable carboxylate–metal interactions. Only two possible electron density features were consistent with proposed metal sites; Fig. 1*A* shows the surroundings of the two metal cations [designated metal sites (M) for the native enzyme]. The site M1 shows nearly ideal octahedral coordination with oxygen atoms from Glu-181, Glu-217, Asp-245, Asp-287, and two water molecules. The second metal site, M2, has a more distorted octahedral coordination and is liganded by three carboxylates (Glu-217, Asp-255, and Asp-257), by His-220 and one water molecule. The carboxylate group of Asp-255 behaves as a bidentate ligand and His-220 is coordinated by atom $N^{\epsilon 2}$. The two metal cations are 4.9 Å apart in the native structure and Glu-217 is coordinated to both cations by different oxygens of its carboxylate group.

The identities of metal ions in the active site were inferred from the magnitudes of the temperature factors and from peak heights in the electron density maps. Mn^{2+} cations in native enzyme crystals have been replaced by the Mg^{2+} used to stabilize the crystals. The coordination geometries for Mn^{2+} and Mg^{2+} are very similar (29, 30) facilitating such an exchange. In the enzyme–D-xylose complex, the two cations appear to be Mn^{2+}. The cation coordination remains the same as in the native structure except that the two water molecules bound to the M1 site have been replaced by O^3 and O^5 of the

sugar molecule as shown in Fig. 1*B*. The distance of 8.3 Å for substrate C^1 to M2 is near the value of 9.1(7) Å reported from NMR studies (31) for C^1-H · · · Mn for the enzyme–xylose complex. In the enzyme–inhibitor complex, the cations again appear to be Mn^{2+}. The metal coordination is unchanged by alkylation except that the two water molecules bound to M1 in the native enzyme have been replaced by O^1 and O^5 of the inhibitor as shown in Fig. 1*C*.

Active Site with Substrate. The active-site region has been identified by the use of difference maps for crystals soaked in D-xylose, as shown in Fig. 1*B*. For clarity, only the density around the substrate is shown. The most striking feature of these difference density maps is that the substrate molecule appears in an "open-chain" conformation rather than the cyclic hemiacetal conformation normally found for free sugars. To our knowledge, this is the first time such a conformation has been observed. The substrate is liganded to the M1 site by O^3 and O^5. The O^3 of the substrate also forms a hydrogen bond to the carboxylate oxygen atom of Glu-181 that is not bound to M1 while O^4 forms a hydrogen bond with

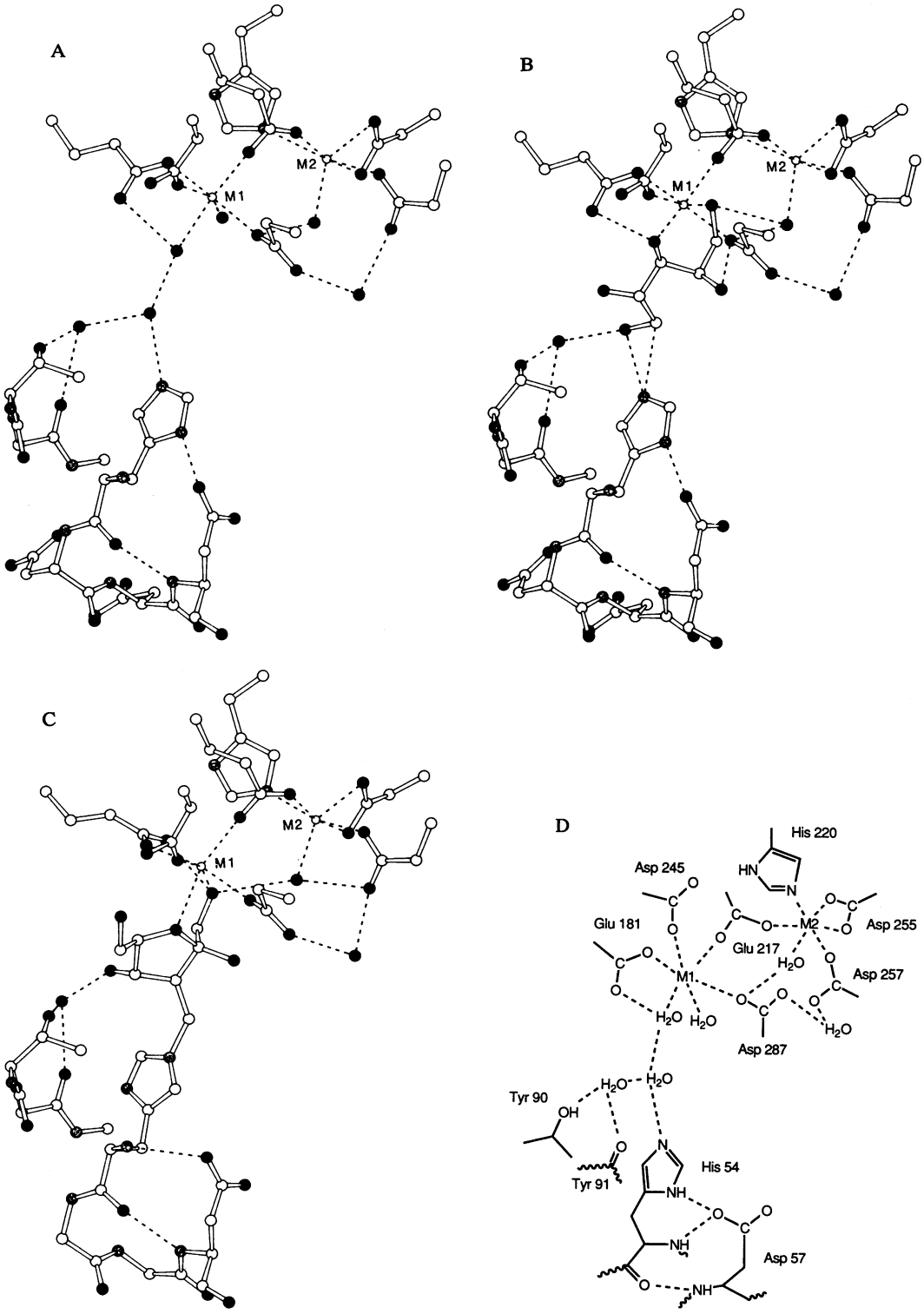

FIG. 1. (*Figure continues on the opposite page.*)

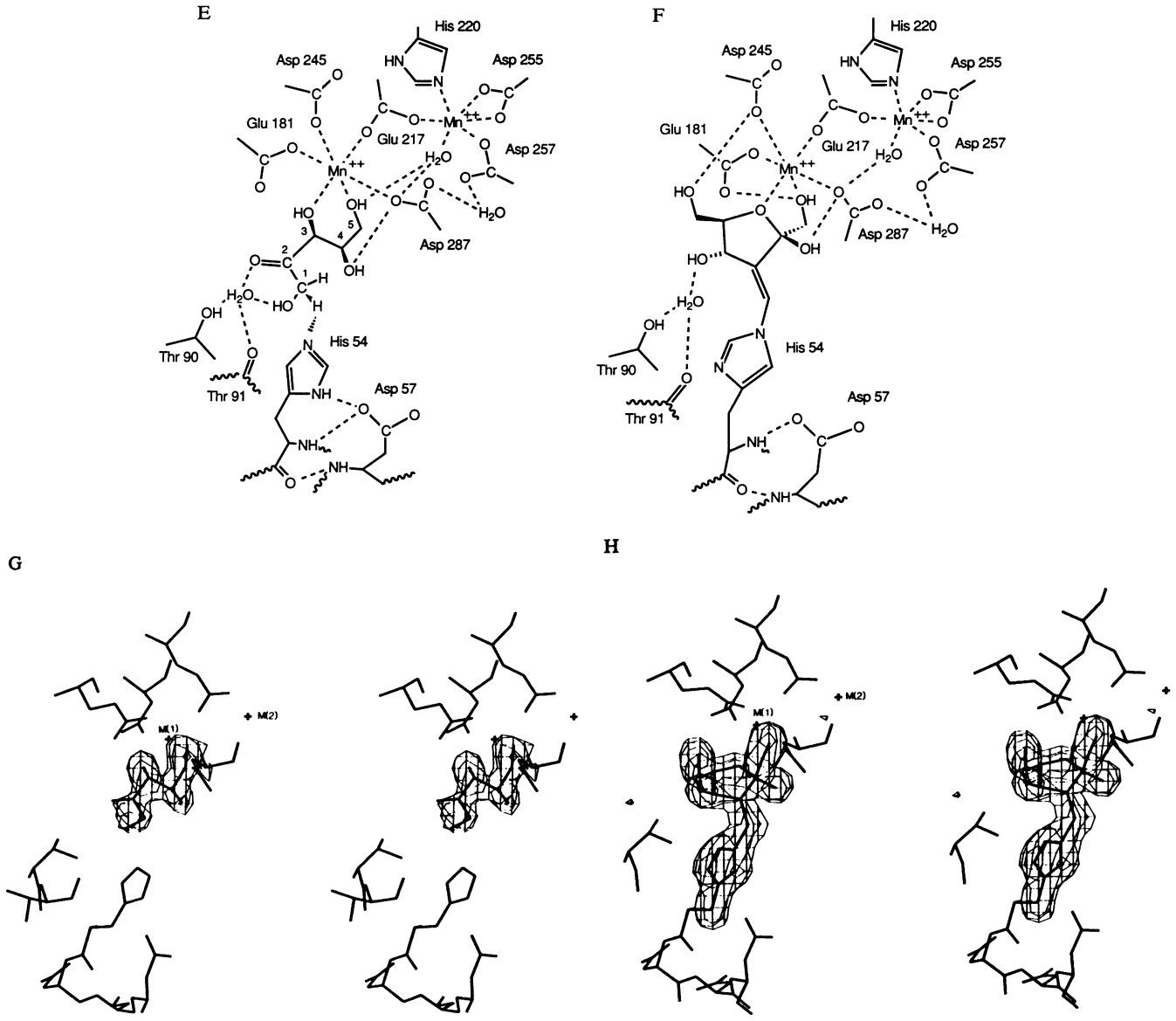

FIG. 1. Ball-and-stick diagrams and chemical formulae of the active site in native enzyme with bound metal (*A* and *D*), enzyme–metal–substrate complex (*B* and *E*), and metal–enzyme–inactivator complex (*C* and *F*) (see ref. 21). Stereoviews of portions of difference electron density maps shown with bound substrate (*G*) and the alkylation product (*H*). The electron density level shown corresponds to 0.3 $e^-/Å^3$.

Asp-287. The O^5 of the substrate forms a hydrogen bond with the water molecule bound to M2. The result is that the substrate is tightly bound by O^3, O^4, and O^5 while the reactive end, O^1 and O^2, is bound through a water molecule to the hydroxyl group of Thr-90. The substrate is oriented with its hydrophobic surface toward Trp-137 and its alignment is also facilitated by Phe-94 from the same subunit and by Phe-26 from another subunit.

Active Site with Mechanism-Based Inhibitor, Analog 2. The D-xylose isomerase from *S. rubiginosus* was inactivated by the two glucose analogs **1** and **2** with pseudo-first-order kinetics (for analog **1**, K_D = 1.5 M and k_{inact} = 0.13 min^{-1}; for analog **2**, K_D = 0.35 M and k_{inact} = 0.18 min^{-1}). Xylitol (20 mM), a competitive inhibitor of normal catalysis (32), reduced the inactivation rate suggesting that the active site is involved in this inactivation. No activity could be restored upon dialysis of the totally inactivated samples. A ^{19}F NMR study of the inactivation of enzyme (1.3 μmol subunit concentration) by analog **2** (3.2 μmol in buffer; total volume, 0.5 ml; 0.01 M $MgCl_2$, at 40°C) gave a signal corresponding to inorganic fluoride (≈1:1 stoichiometry with respect to the enzyme). No other signals appeared. Therefore, the partition ratio with analog **2**, defined as the ratio of the number of times a substrate turns over (inactivation included) to each inactivation event (33), is nearly 1.0, indicating that, after turnover, analog **2** immediately inactivates the enzyme (presumably by formation of a covalent bond). Thus, analog **2** can be considered a mechanism-based inactivator (Scheme **1**) (34). Addition of a nucleophile (5 mM cysteine) completely protected the enzyme from inactivation by analog **1** but had no effect on the inactivation by analog **2** (0.4 M). The protection against analog **1** (which is not a mechanism-based inactivator) implies that its reaction product dissociates before the enzyme inactivation, whereas analog **2** is converted by isomerization to an inactivating species that acts before any dissociation. The fluorine substitution in analog **2** has increased the electrophilicity of the α,β-unsaturated ketone so that the inactivation, in this case, occurs from a binary enzyme–α,β-unsaturated ketone complex.

Difference maps for crystals soaked in analog **2** clearly showed the location of each atom in the ternary enzyme–metal–inhibitor complex as illustrated in Fig. 1*C*. The compound **2** has alkylated $N^{\epsilon 2}$ of His-54 and as a result, the histidine ring has rotated 180° about χ_2 and 15° about χ_1 and

the carboxylate group of Asp-57 is no longer hydrogen-bonded to it. The inhibitor, in a cyclic form, replaces the two water molecules on M1 of native enzyme (the positions of O^3 and O^5 of the substrate). Another hydroxyl group of analog **2** binds to the water that binds O^1 and/or O^2 of the substrate.

CONCLUSIONS

We have established the mode of binding of substrate on the enzyme, located the two metal sites, and identified the nature of the inactivation product obtained by the reaction of enzyme with analog **2** (Fig. 1). The water molecules in the native enzyme are systematically replaced by hydroxyl groups when substrate or analog **2** bind to the enzyme. The substrate, aligned by phenylalanine and tryptophan side chains, is bound to enzyme by Mn^{2+} in the unusual open-chain form. There is a close interaction of C^1 of the substrate with His-54, indicating an incipient hydrogen abstraction through the re-face of C^1, and the oxygen atoms on C^1 and C^2 are near to a water molecule that is held in place by Thr-90 and Thr-91. This suggests that the base catalyst in the enzymatic reaction is His-54 and that the water molecule near O^1 and O^2 of the substrate might be presumed to be the acid catalyst that polarizes the carbonyl group of the substrate that in turn facilitates the formation of an ene-diol intermediate. Our results are consistent with the reaction stereospecificity (2), that is, re-face abstraction, transfer, and a cis-ene-diol mechanism. The role of the metal ions (Mn^{2+} preferred) appears to be twofold. They maintain the structural integrity of the active site and, in the tight metal-binding site M1, stabilize the open-chain form of the substrate sugar by binding the hydroxyl groups at the end of the molecule most distant from the site of the isomerization reaction.

The alkylation of His-54 by the suicide inactivator, analog **2**, serves to reinforce the interpretation that His-54 is the base catalyst. It also confirms that the enzyme is in an active state, because, in these crystals, a glucose analog has been converted to the cyclic fructose analog studied here. Presumably inactivation occurs with the open form of analog **2** and cyclization follows the isomerization reaction. Either study alone (with D-xylose or with analog **2**) would have been sufficient to locate the active site and to identify the base catalyst. The fact that both studies give the same result clearly indicates the features of the active site that are illustrated in Fig. 1.

The authors in Strasbourg dedicate this article to the memory of Prof. E. Lederer (1908–1988). Samples of enzymes were generously provided to the Philadelphia group by Drs. R. Antrim and N. Lloyd of Nabisco Brands, and to the Strasbourg group by the firm A. Arnaud (Paris) as Spezyme GI, Finn sugar group. We thank Drs. G. D. Markham, H. M. Berman, M. Lewis, and R. E. Johnson for much assistance. We thank H. Wong and R. Drummond of Cetus Corporation for the amino acid sequence prior to publication. Coordinates of α-carbon atoms have been deposited with the Protein Data Bank. Coordinates of all atoms (for the three structures) will be deposited when the full structure is reported elsewhere. This research was funded by Grants CA-10925, CA-06927, and RR-05539 from the National Institutes of Health; in the early stages by Grant PCM74-21036 from the National Science Foundation; and by an appropriation from the Commonwealth of Pennsylvania.

1. Hochster, R. M. & Watson, W. A. (1953) *J. Am. Chem. Soc.* **75,** 3284–3285.
2. Rose, I. A., O'Connell, E. L. & Mortlock, R. P. (1969) *Biochem. Biophys. Acta* **178,** 376–379.
3. Schray, K. J. & Rose, I. A. (1971) *Biochemistry* **10,** 1058–1062.
4. Schray, K. J. & Mildvan, A. S. (1972) *J. Biol. Chem.* **247,** 2034–2037.
5. Berman, H. M., Rubin, B. H., Carrell, H. L. & Glusker, J. P. (1974) *J. Biol. Chem.* **249,** 3983–3984.
6. Carrell, H. L., Rubin, B. H., Hurley, T. J. & Glusker, J. P. (1984) *J. Biol. Chem.* **259,** 3230–3236.
7. Henrick, K., Blow, D. M., Carrell, H. L. & Glusker, J. P. (1987) *Protein Eng.* **1,** 467–469.
8. Muirhead, H. (1983) *Trends Biochem. Sci.* **8,** 326–330.
9. Magnien, A., LeClef, B. & Biellmann, J. F. (1984) *Biochemistry* **23,** 6858–6862.
10. Anderson, F. & Samuelson, B. (1984) *Carbohydr. Res.* **129,** C1–C3.
11. Kartha, K. P. R. (1986) *Tetrahedron Lett.* **27,** 3415–3416.
12. Fitzer, L. & Quabeck, C. V. (1985) *Synth. Commun.* **15,** 855–864.
13. Burton, D. J. & Wiemers, D. M. (1985) *J. Fluorine Chem.* **27,** 85–89.
14. Schlosser, M. & Christmann, K. F. (1967) *Liebigs Ann. Chem.* **708,** 1–35.
15. Koch, H. J. & Perlin, A. S. (1970) *Carbohydr. Res.* **15,** 403–410.
16. Rosenthal, A. & Sprinzl, M. (1969) *Can. J. Chem.* **47,** 3941–3948.
17. Tronchet, J. M. J., Schwarzenbach, D. & Barbalat-Rey, F. (1976) *Carbohydr. Res.* **46,** 9–17.
18. Dische, Z. & Borenfreund, E. (1951) *J. Biol. Chem.* **192,** 583–587.
19. Howard, A. J., Gillilano, G. L., Finzel, B. C., Poulos, T. L., Ohlendorf, D. H. & Salemme, F. R. (1987) *J. Appl. Crystallogr.* **20,** 383–387.
20. Wang, B. C. (1985) *Methods Enzymol.* **115,** 90–112.
21. Drocourt, D., Bejar, S., Calmels, T., Reynes, J. P. & Tiraby, G. (1988) *Nucleic Acids Res.* **16,** 9337.
22. Jones, T. A. (1978) *J. Appl. Crystallogr.* **11,** 268–272.
23. Carrell, C. J., Carrell, H. L., Erlebacher, J. & Glusker, J. P. (1988) *J. Am. Chem. Soc.* **110,** 8651–8656.
24. Hendrickson, W. A. & Konnert, J. H. (1980) in *Computing in Crystallography,* eds. Diamond, R., Ramaseshan, S. & Venkatesan, K. (Indian Acad. Sci., Bangalore, India), pp. 13.01–13.25.
25. Hendrickson, W. A. (1985) *Methods Enzymol.* **115,** 252–270.
26. Ten Eyck, L. F. (1977) *Acta Crystallogr. Sect. A* **33,** 486–492.
27. Knossow, M., Lewis, M., Rees, D., Wilson, I. A., Skehel, J. J. & Wiley, D. C. (1986) *Acta Crystallogr. Sect B* **42,** 627–632.
28. Luzzati, V. (1952) *Acta Crystallogr.* **5,** 802–810.
29. Johnson, C. K. (1965) *Acta Crystallogr.* **18,** 1004–1018.
30. Glusker, J. P. & Carrell, H. L. (1973) *J. Mol. Struct.* **15,** 151–159.
31. Young, J. M., Schray, K. J. & Mildvan, A. S. (1975) *J. Biol. Chem.* **250,** 9021–9027.
32. Noltmann, E. A. (1972) in *The Enzymes,* ed. Boyer, P. D. (Academic, New York), Vol. 6, pp. 349–354.
33. Wang, E. & Walsh, C. T. (1978) *Biochemistry* **17,** 1313–1321.
34. Abeles, R. H. & Maycock, A. L. (1976) *Acc. Chem. Res.* **9,** 313–319.